American Mineralogist, Volume 58, pages 756–764, 1973

Effect of Variations in O-P-O and P-O-P Angles on P-O Bond Overlap Populations for Some Selected Ortho- and Pyrophosphates

GEORGE A. LAGER,[1] AND G. V. GIBBS
Department of Geological Sciences
Virginia Polytechnic Institute and State University
Blacksburg, Virginia 24061

Abstract

Extended Hückel molecular orbital (EHMO) calculations for hypothetically distorted PO_4^{3-} and $P_2O_7^{4-}$ ions predict that shorter P–O bonds on the average should be involved with wider P–O–P and O–P–O angles. Plots of P–O bond length *vs* the average of the three O–P–O angles common to each bond, and of ⟨P–O(br)⟩ *vs* P–O–P angle, confirm this for selected ortho- and pyrophosphates. Bond overlap populations, *n*[P–O], calculated with all P–O bond lengths clamped at 1.50 Å, tend to be larger for shorter observed P–O bond lengths. The P–O bond lengths in herderite, $CaBePO_4(OH)$, are estimated from EHMO theory using a relation between bond overlap population and bond length. As ζ(O), *n*[P–O], bond number and π-bond order are highly correlated, caution should be exercised in making inferences about the nature of a bond because any one of these parameters appears capable of providing a plausible interpretation of bond length and angle variations. It appears that both ζ(O) and *n*[P–O] measure a similar property of the P–O bond.

Introduction

In 1939, Pauling proposed that phosphorus may utilize its outer 3*d*-orbitals in a double-bond formation with its coordinating oxygen atoms because it is not rigorously restricted by the octet rule. Expanding upon this proposal, Cruickshank (1961) has asserted from group-theory arguments and approximate molecular orbital calculations that only two of the five 3*d*-orbitals, $3d_{x^2-y^2}$ and $3d_{z^2}$, are actually used in double-bond formation in PO_4 tetrahedra. Employing a model for establishing bond strengths, he worked out the π-bond orders for the tetrahedral bonds in a number of phosphates and found that they correlate well with the observed P–O bond lengths. Cruickshank predicted from his model that: (1) P–O(nbr) bonds should be shorter than P–O(br) bonds and (2) the length of the P–O(br) bond should increase as the P–O–P angle decreases. Brown and Gibbs' (1970) scatter diagrams of ⟨P–O(br)⟩ and of [⟨P–O(br)⟩–⟨P–O(nbr)⟩] versus P–O–P angle apparently substantiate both predictions. Recently Baur (1970) demonstrated that the steric details in phosphates can also be rationalized in terms of his extended electrostatic model.

In an extended Hückel molecular orbital (EHMO) examination of the Pauling-Cruickshank *d-p* π-bonding model, Bartell, Su, and Yow (1970) have found that Mulliken bond overlap populations, *n*[P–O], calculated for a number of phosphates correlate with the simple π-bond orders worked out by Cruickshank (1961). They observed good correlation between P–O bond length and *n*[P–O] even though all P–O distances were held constant at 1.50 Å during the calculations. They also conclude that all five 3*d*-orbitals participate in bonding instead of just the two as proposed by Cruickshank (1961).

The present study (Lager, 1972; Lager and Gibbs, 1972) was undertaken to evaluate the effect of the variations in the O–P–O and P–O–P angles on *n*[P–O] and P–O bond length, relationships not considered by Bartell *et al* (1970). Evidence will be presented which will show that *n*[P–O] values are strongly dependent upon angular variations indicating that shorter P–O bonds on the average should be involved in wider O–P–O and P–O–P angles. In addition, the similarities between bonding models and parameters will be discussed.

Correlations Between Bond Overlap Population and P–O Bond Length

The phosphates selected in our study are given in Table 1 together with their calculated Mulliken (1955) bond overlap populations, *n*[P–O], and ob-

[1] Now at the Department of Geology, University of British Columbia, Vancouver 8, British Columbia, Canada.

TABLE 1. Observed bond lengths and calculated bond overlap populations for selected phosphates.

	(P–O)Å		n(P–O)	
Bond	P–O(br)	P–O(nbr)	P–O=1.50	P–O=obs
	α-$Mg_2P_2O_7$ (Calvo, 1967)			
P(1)–O(1)	1.613		0.620	0.556
P(1)–O(2)		1.535	.642	.625
P(1)–O(3)		1.506	.641	.648
P(1)–O(4)		1.473	.654	.687
P(2)–O(1)	1.568		.624	.599
P(2)–O(5)		1.535	.647	.631
P(2)–O(6)		1.526	.637	.630
P(2)–O(7)		1.521	.648	.645
	α-$Ca_2P_2O_7$ (Calvo, 1968)			
P(1)–O(1)	1.579		0.621	0.587
P(1)–O(2)		1.518	.650	.645
P(1)–O(3)		1.521	.641	.634
P(1)–O(4)		1.507	.637	.643
P(2)–O(1)	1.616		.618	.556
P(2)–O(5)		1.535	.648	.633
P(2)–O(6)		1.508	.642	.649
P(2)–O(7)		1.493	.642	.662
	β-$Ca_2P_2O_7$ (Webb, 1966)			
P(1)–O(1)	1.637		0.610	0.541
P(1)–O(2)		1.505	.638	.654
P(1)–O(3)		1.538	.647	.632
P(1)–O(4)		1.519	.653	.655
P(2)–O(1)	1.615		.610	.554
P(2)–O(5)		1.480	.644	.675
P(2)–O(6)		1.530	.645	.633
P(2)–O(7)		1.526	.650	.641
P(3)–O(8)	1.589		.621	.581
P(3)–O(9)		1.498	.649	.665
P(3)–O(10)		1.504	.647	.657
P(3)–O(11)		1.563	.639	.602
P(4)–O(8)	1.618		.611	.551
P(4)–O(12)		1.503	.639	.654
P(4)–O(13)		1.527	.651	.644
P(4)–O(14)		1.527	.651	.645
	α-$Cu_2P_2O_7$ (Robertson and Calvo, 1967)			
P(1)–O(1)	1.578		0.639	0.597
P(1)–O(2)		1.533	.632	.615
P(1)–O(3)		1.478	.641	.669
P(1)–O(4)		1.517	.649	.644
P(2)–O(1)	1.580		.625	.594
P(2)–O(5)		1.546	.642	.624
P(2)–O(6)		1.562	.640	.609
P(2)–O(7)		1.518	.653	.657
	β-$Zn_2P_2O_7$ (Calvo, 1965b)			
P(1)–O(1)	1.569		0.640	0.616
P(1)–O(2)		1.554	.633	.612
P(1)–O(3)		1.553	.646	.625
P(1)–O(4)		1.553	.646	.625
P(2)–O(1)	1.569		.640	.616
P(2)–O(5)		1.554	.633	.613
P(2)–O(6)		1.555	.646	.623
P(2)–O(7)		1.555	.646	.623
	$Ca_7Mg_9(Ca,Mg)_2(PO_4)_{12}$ (Dickens & Brown, 1971)			
P(1)–O(1)		1.563	0.628	0.594
P(1)–O(2)		1.521	.636	.635
P(1)–O(3)		1.521	.648	.647
P(1)–O(4)		1.554	.628	.602
P(2)–O(5)		1.534	.639	.627
P(2)–O(6)		1.525	.638	.634
P(2)–O(7)		1.527	.639	.633
P(2)–O(8)		1.568	.624	.587
P(3)–O(9)		1.528	.642	.636
P(3)–O(10)		1.577	.624	.581
P(3)–O(11)		1.530	.639	.632
P(3)–O(12)		1.528	.635	.630
P(4)–O(13)		1.539	.632	.617
P(4)–O(14)		1.538	.639	.625
P(4)–O(15)		1.539	.640	.624
P(4)–O(16)		1.539	.629	.615
P(5)–O(17)		1.546	.638	.617
P(5)–O(18)		1.549	.627	.604
P(5)–O(19)		1.521	.642	.640
P(5)–O(20)		1.530	.633	.624
P(6)–O(21)		1.523	.628	.624
P(6)–O(22)		1.528	.635	.627
P(6)–O(23)		1.535	.635	.621
P(6)–O(24)		1.545	.642	.619
	Herderite (Lager & Gibbs, in preparation)			
P(1)–O(1)		1.513	0.642	0.648
P(1)–O(2)		1.544	.636	.617
P(1)–O(3)		1.551	.634	.610
P(1)–O(4)		1.554	.630	.604

TABLE 2. Valence orbital ionization potentials (VOIP) and orbital exponents (ζ).

Atom	Atomic Orbital	VOIP(ev)	ζ
Oxygen	2s	-35.13	2.275
	2p	-13.62	2.275
Phosphorus	3s	-20.30	1.600
	3p	-11.00	1.600
	3d	-2.50	1.100

served P–O bond lengths. Values of *n*[P–O] were calculated using the EHMO program written by Hoffmann (1963), the orbital exponents and diagonal Hückel matrix elements given in Table 2, and the Wolfsberg-Helmholz parametrization (*cf* Bartell *et al,* 1970). The relationship between observed P–O bond length and *n*[P–O] calculated using constant bond lengths (1.50 Å), observed O–P–O and P–O–P angles, and an *sp* basis set is shown in Figure 1. A plot of observed P–O lengths versus *n*[P–O] values calculated using the observed bond lengths and angles (Fig. 2) gives a statistically improved correlation as expected. Although *n*[P–O] values calculated using an *spd*-basis set also correlate with P–O bond length (Bartell *et al,* 1970; Lager, 1972), the correlations are not given because comparisons of all electron *ab initio* SCF-MO and EHMO results show that EHMO calculations tend to over-exaggerate the participation of the *d*-orbitals in the resulting MO wavefunctions (Leland Allen, personal communication).

Correlations Between O–P–O and P–O–P Angles and *n*[P–O]

The correlations obtained between observed P–O bond lengths and *n*[P–O] values calculated with fixed P–O distances indicate that the O–P–O and P–O–P angles affect bond overlap population. To evaluate this effect, EHMO calculations were carried out on hypothetically distorted PO_4^{3-} and $P_2O_7^{4-}$ ions. The P–O distances were fixed in the calculations at 1.50 Å and the angles were varied over a range which was thought to be consistent with experimentally observed values. A minimum valence *sp* basis set was assumed in all the calculations. The calculated trends were then compared with observed data obtained for the phosphates in Table 1.

O–P–O *angle vs n*[P–O]

In the calculation for the hypothetically distorted PO_4^{3-} ion, the basal (β) and apical (α) angles were varied within the constraints of C_{3v} symmetry (see

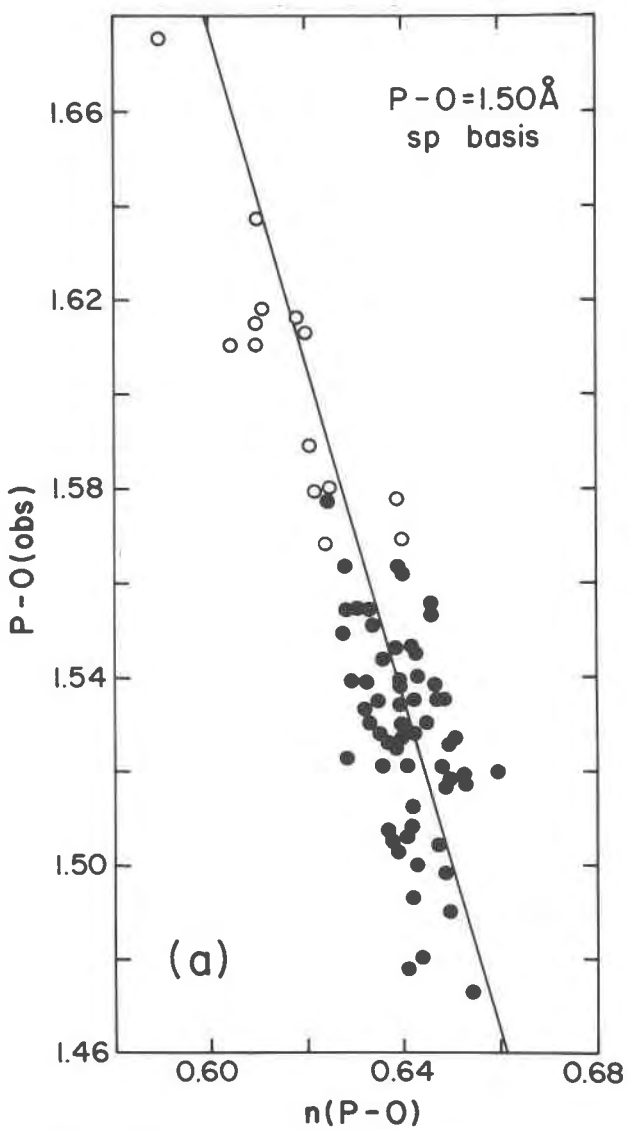

FIG. 1. Scatter diagram of observed P–O bond lengths *vs* n(P–O) calculated ignoring the non-tetrahedral cations, using observed O–P–O and P–O–P angles and assuming all P–O bonds are 1.50Å in length. Open circles refer to P–O(br) bonds and the solid ones, P–O(nbr) bonds. Data from Table 1.

insert, Fig. 3). Values of n[P–O] calculated for seven different α angles between 102° and 117° indicate that as the apical angle (α) widens, n[P–O(apical)] increase while n[P–O(basal)] decrease (Fig. 3). Accordingly, when α is larger than β, the apical bond is predicted to be shorter than the basal bonds. It is encouraging to find that the steric details predicted by EHMO theory (Fig. 3) are consistent with the relationship between $\langle$O–P–O$\rangle_3$, the mean of the three tetrahedral angles common to a bond, and observed P–O bond length (Fig. 4a) and n[P–O] (Fig. 4b). This suggests that part of the P–O bond length *vs* O–P–O angle variation can be interpreted in terms of the predominantly covalent EHMO model (*cf* Bartell *et al*, 1970).

P–O–P *angle vs* n[P–O]

In a model which requires the participation of *s*- and *p*-orbitals in bond formation, shorter P–O(br) bonds are predicted to be involved with wider P–O–P angles. In order to test this prediction, the effect of the O–P–O angles must also be considered because n[P–O(br)] will depend on angular variations within a tetrahedron (*vide supra*). This is evident from an examination of the n[P–O] values calculated with all P–O = 1.50 Å for the three $P_2O_7^{4-}$ ions (D_{3h} point symmetry) depicted in Figure 5 where O(br)–P–O(nbr) angles are set at (a) 117°, (b) 109.47°, and (c) 102°, respectively. Because of the intrinsic relation between n[P–O(br)] and O–P–O angle, EHMO calculations were carried out on $P_2O_7^{4-}$ ions (Fig. 5) in which both O(br)–P–O(nbr) and P–O–P angles were varied. The results (Fig. 6) indicate that regardless of whether the O(br)–P–O(nbr) is

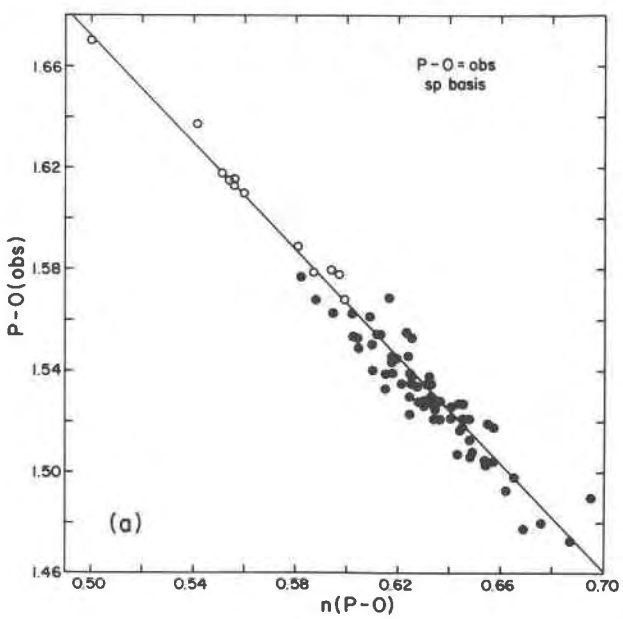

FIG. 2. Scatter diagram of observed P–O bond lengths *vs* n(P–O) calculated using observed angles and bond lengths but ignoring the non-tetrahedral cation for compounds in Table 1. Open circles designate P–O(br) bonds and closed ones P–O(nbr) bonds.

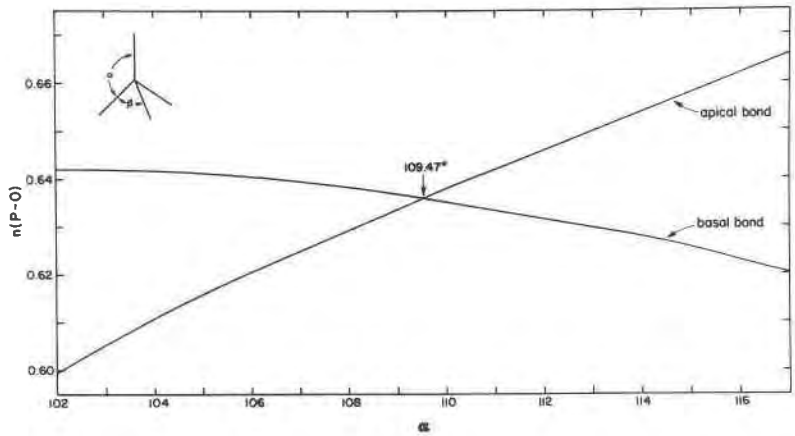

FIG. 3. Plot of O–P–O angle *vs* n(P–O) for the apical and basal bonds in a phosphate ion with C_{3v} point symmetry. The n(P–O) were calculated with all P–O bond lengths fixed at 1.50Å using a minimum *sp* basis set. α defines the O–P–O angles between the P–O apical bond parallel to C_3 and the basal bonds in vertical mirrors, σ_v, and β defines the O–P–O angles between the P–O bonds lying in σ_v (see insert in upper left corner).

greater or less than 109.47°, n[P–O(br)] values exhibit an inverse relationship with respect to the P–O–P angle, with the largest n[P–O(br)] always associated with the widest angle. This is consistent with the plot of ⟨P–O(br)⟩ *vs* P–O–P prepared by Brown and Gibbs (1970), with observations by Cruickshank (1961) and by Calvo (1965a, b) and with the data in Figure 7 where the average observed P–O bond length, ⟨P–O(br)⟩, is plotted as a function of associated P–O–P angle.

Bond Length Estimates from Ehmo Theory

A linear equation for estimating P–O bond lengths, similar to that developed by Baur (1970), can be deduced from the relationship (*cf* Mulliken, 1955; Louisnathan and Gibbs, 1972)

$$\frac{\Delta n[\text{P–O}]}{n_e[\text{P–O}]} = \frac{\Delta d(\text{P–O})}{d_e(\text{P–O})} \qquad (1)$$

where n_e[P–O] represents the P–O bond overlap population calculated for each bond in an ideal PO_4^{3-}

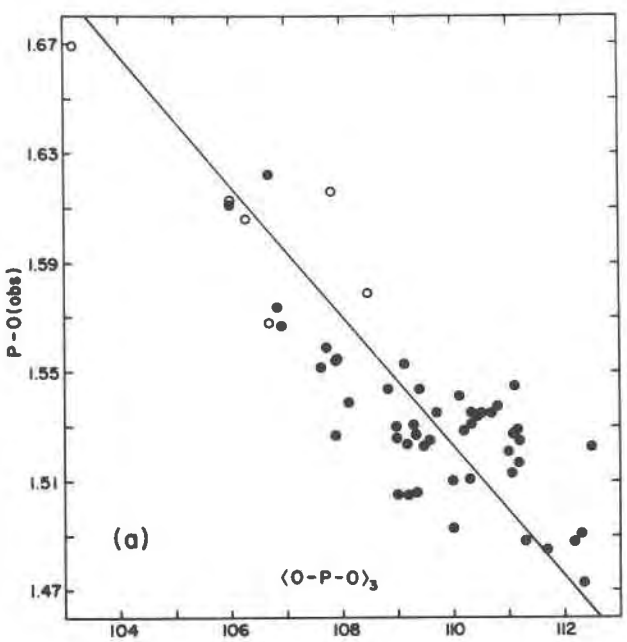

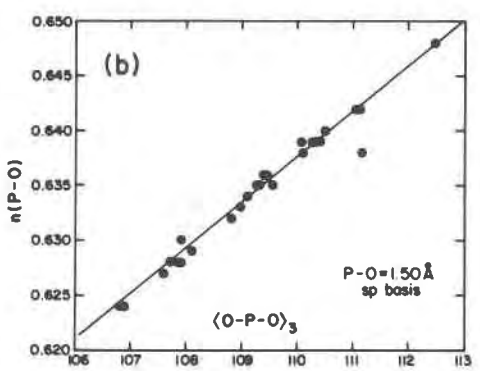

FIG. 4. Scatter diagram of ⟨O–P–O⟩$_3$ (= the average O–P–O angle involving a common P–O bond) *vs* (a) the observed P–O bond length and (b) n(P–O) calculated assuming a constant bond length of 1.50Å, using the observed angles and ignoring the non-tetrahedral cations. Data for (a) are from the following sources in addition to Table 1: $Na_5P_3O_{10}$, Phase II, (Cruickshank, 1964b); $RbPO_3$, (Cruickshank, 1964e). Data for plot (b) are from $CaBePO_4F$ and $Ca_7Mg_9(Ca,Mg)_2(PO_4)_{12}$.

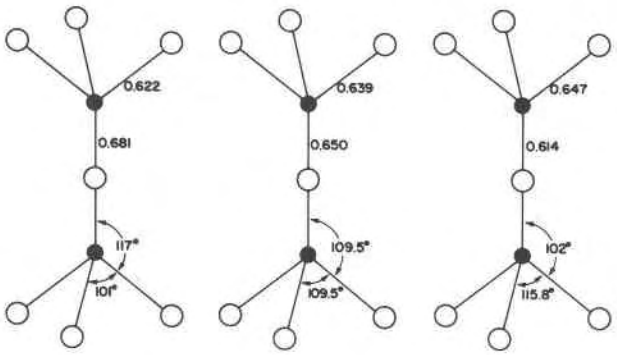

FIG. 5. A comparison of n(P–O) (values given adjacent to P–O(br) and P–O(nbr) bonds in upper part of each ion) calculated for three pyrophosphate ions, $P_2O_7^{4-}$, (with D_{3h} point symmetry with straight P–O(br)–P linkage along C_3) where in (a) the O(br)–P–O(nbr) angles are wider than the O(nbr)–P–O(nbr), (b) the O(br)–P–O(nbr) angles are equal to O(nbr)–P–O(nbr) angles and (c) the O(br)–P–O(nbr) angles are narrower than the O(nbr)–P–O(nbr) angles. The calculations were made using all P–O bond lengths clamped at 1.50Å and the O–P–O angles indicated at the lower part of each ion.

tetrahedron (T_d symmetry) assuming an equilibrium bond length d_e(P–O) of 1.50 Å and where Δd(P–O) is the change in the bond length associated with a change in the overlap population, Δn[P–O]. To obtain estimates of individual P–O bond lengths induced by changes in the bond overlap population, we can write that

$$\text{P–O(est.)} = d_e\text{(P–O)} + \Delta d\text{(P–O)}.$$

Replacing Δd(P–O) by (1) and d_e(P–O) by ⟨P–O⟩, the grand mean P–O bond length (1.538 Å) found for a large number of phosphates (Louisnathan and Gibbs, 1972), we have that

$$\begin{aligned}\text{P–O(est.)} &= \langle\text{P–O}\rangle + b\Delta n\text{[P–O]} \\ &= 1.538 + 2.479\ \Delta n\text{[P–O]} \qquad (2)\end{aligned}$$

where the slope of the line

$$b = \frac{d_e\text{(P–O)}}{n_e\text{[P–O]}} = \frac{1.500}{0.636} = 2.479$$

and where ⟨P–O⟩ is the intercept.

To learn whether equation (2) is consistent with the data given in Table 1, Δn[P–O] = n_e[P–O] – n[P–O] was plotted against the observed P–O bond lengths (Fig. 8) where n[P–O] is the bond overlap population calculated assuming P–O = 1.50 Å. The regression line fitted to the data

$$\text{P–O(est.)} = 1.545 + 4.192\ \Delta n\text{[P–O]}$$

is in fair agreement with (2), suggesting that the latter can be used to make *crude* estimates of the tetrahedral bond lengths in phosphates.

The P–O bond lengths in herderite, $CaBePO_4F$, estimated using equation (2), show a reasonable correspondence with those observed (see Table 3). Bond lengths estimated from Baur's equation P–O(est.) = 1.537 + 0.109$\Delta\zeta$(O)[2] have been included for comparison. However, the purpose of this comparison is *not* to show that equation (2) is superior in any way to Baur's but to show that the two are remarkably similar and that they give comparable estimates. This is true despite the fact that Baur's equation is based on an electrostatic parameter, $\Delta\zeta$(O), while equation (2) is based on a covalent parameter, Δn[P–O]. Accordingly, it is clear that one should be circumspect in concluding that a bond is predominantly ionic in character because $\Delta\zeta$(O) can be used to estimate bond length variations (*vide post*).

Discussion

Since Pauling (1929) formulated his empirical set of rules for complex ionic compounds, the steric details of many structures have been found to be consistent with his simple electrostatic model. Baur (1970) has examined the phosphates and a number of other compounds in terms of Pauling's model and has found that ζ(O) correlates well with observed bond lengths. Interestingly, the bond lengths for the crystal structures examined by Baur show two apparent populations when plotted as a function of ζ(O), with the bond lengths involving oxygen and mono- or divalent cations giving distinctively poorer correlations than those involving oxygen and tri- or tetravalent cations. Baur (1970) suggests that, "this is partly due to the fact that in most of the crystal structures from which data have been used, the mono- and divalent cations form the weaker bonds . . .". Nevertheless, he is careful to note that the correlations could also be interpreted in terms of Cruickshank's double-bonding model. This observation is evinced by Figure 9, which shows that the ζ(O) values for the phosphates studied by Cruick-

[2] $\Delta\zeta$(O) = ζ(O) – ⟨ζ(O)⟩ where ζ(O) is the sum of the strengths of the electrostatic bonds received by oxygen and ⟨ζ(O)⟩ is the mean ζ(O) for the phosphate ion under consideration.

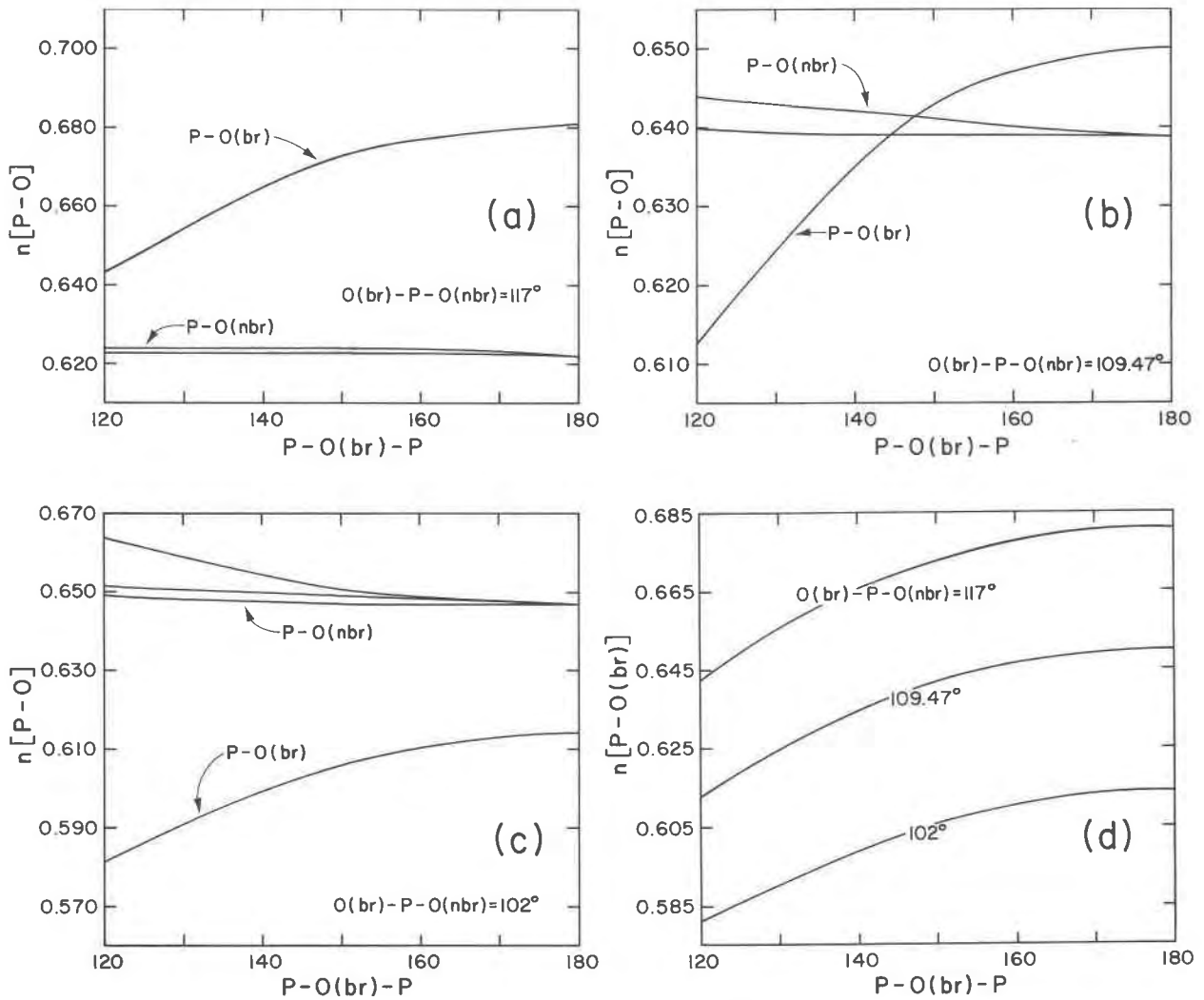

FIG. 6. Curves relating P–O(br)–P angle to n(P–O) calculated for three pyrophosphate ions in Figures 5a, 5b, and 5c, assuming all P–O bond lengths to equal 1.50Å.

shank (1961) are strongly correlated with π-bond order. Moreover, Baur's (1970) results also show that ζ(O) correlates better with bond length variations in the more covalent compounds[3] (P–O, r = 0.87; S–O, r = 0.83; Si–O, r = 0.69; B–O, r = 0.63) than with those in the more ionic ones (Ca–O, r = 0.56; Na–O, r = 0.49; Mg–O, r = 0.38; K–O, r = 0.20), suggesting that ζ(O) is reflecting some covalent aspect of a bond (Pant and Cruickshank, 1967; Gibbs *et al*, 1972; Brown and Shannon, 1973).

In view of the above discussion, it is tempting to speculate on the validity of the correlations of ζ(O) *vs* π-bond order and n[P–O] (Fig. 10). Although an intrinsic relation between these parameters cannot be proven, these correlations are given credence by the well-developed correlation between the group overlap integrals calculated by Jaffe (1954) and the electrostatic bond strengths of the T–O bonds for the four tetrahedral oxyanions depicted in Figure 11. This plot, as well as those of Figures 9 and 10, indicates that the parameters used to characterize bond

[3] The correlation coefficients, r, quoted here were obtained by Baur (1970) in his linear regression analyses of bond length variation *vs* ζ(O). As r^2 is a measure of the percent bond length variation $d(M$–O) that can be explained in terms of a linear dependence on ζ(O), it is evident that more of the variation in $d(M$–O) can be explained for the more electronegative metal atoms than for the more electropositive ones.

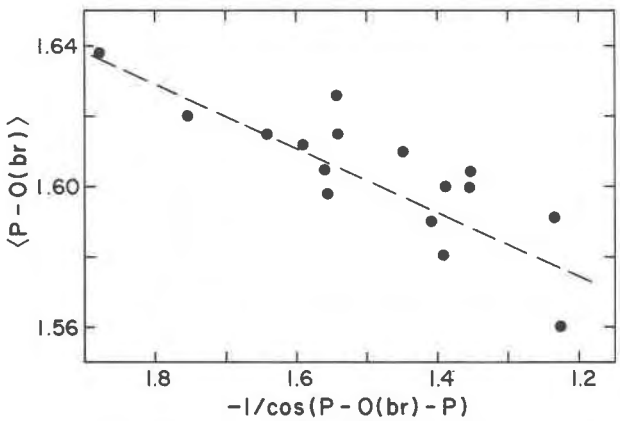

FIG. 7. Scatter diagram of ⟨P–O(br)⟩, the average P–O bond length to the bridging oxygen *vs* $-1/[\cos(\text{P–O(br)–P})]$. Data were taken from Table 1 and from the following sources: $Na_4P_2O_7 \cdot 10H_2O$, Cruickshank, 1964e; $Na_2H_2P_4O_{12}$, Jarchow, 1964; $Na_4P_4O_{12} \cdot 4H_2O$, Ondik, 1964; $(NaPO_3)_z$, McAdam *et al*, 1968; P_2O_5, Cruickshank, 1964d; β-$Mg_2P_2O_7$, Calvo, 1965a; $(NH_4)_4P_4O_{12}$, Cruickshank, 1964c.

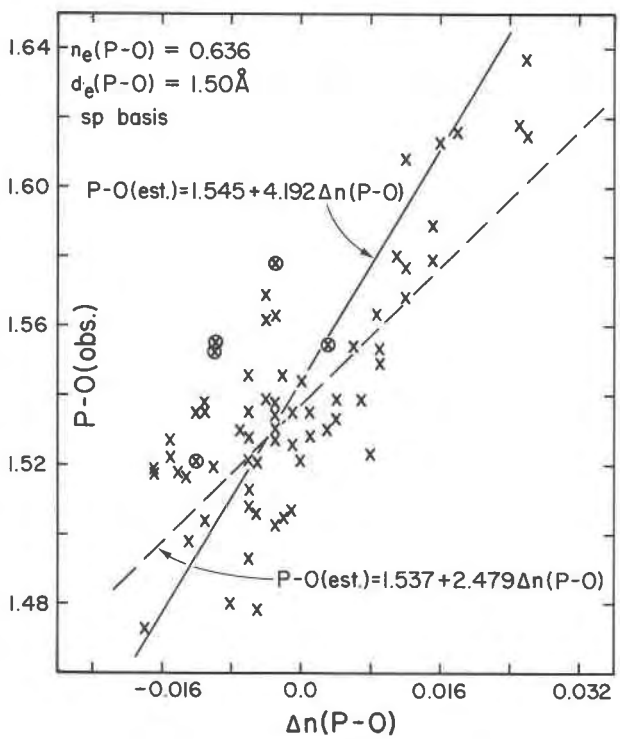

FIG. 8. A scatter diagram of the observed P–O bond length *vs* the variation in the equilibrium bond overlap population, Δn(P–O) calculated assuming constant P–O bond lengths and observed O–P–O and P–O–P angles. Data from Table 1. Encircled-crosses represent two data plots. The expression taken from Mulliken (1955) (dashed line) is compared with the regression line for the data set (solid line). See text for explanation.

TABLE 3. Comparison of observed and estimated P–O bond lengths in herderite, $CaBePO_4(OH)$ (Lager and Gibbs, in preparation).

Bond	P-O(obs)Å	P-O(est.)Å*	P-O(est.)Å**
P-O(1)	1.513(3)***	1.510	1.522
P-O(2)	1.544(3)	1.537	1.537
P-O(3)	1.551(3)	1.564	1.542
P-O(4)	1.554(3)	1.537	1.552

* P-O(est.) = 1.537 + 0.109 $\Delta\zeta$(O) (Baur, 1970)

** P-O(est.) = 1.537 + 2.479 Δn(P-O) (this study)

*** esd's refer to last digit of observed P-O bond length

strengths in current bonding models are very similar indeed. Accordingly, *caution* should be exercised in making inferences about the nature of a bond, because one or the other of these parameters appears capable of providing a plausible interpretation of bond length and angle variations.

In conclusion, we have tried to emphasize the close similarity between the EHMO and the electrostatic bonding models. The steric details in the phosphates, for example, are consistent with the EHMO model and yet many aspects conform remarkably well with electrostatic models (Pauling, 1929; Baur, 1970). This

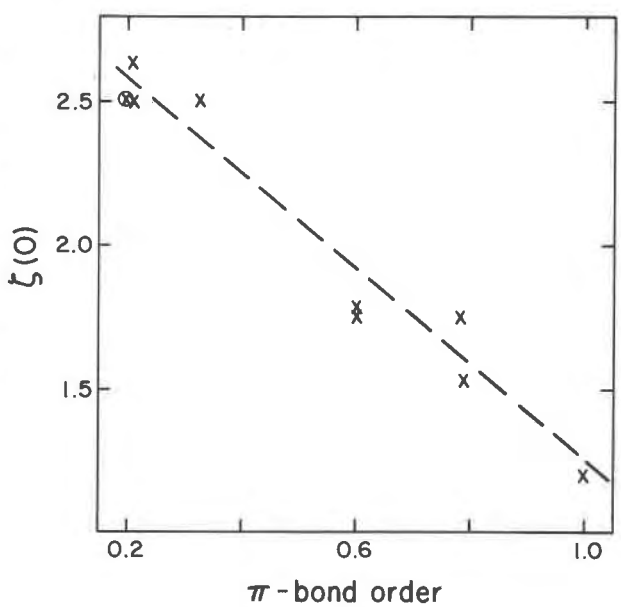

FIG. 9. Scatter diagram of ζ(O) *vs* π-bond orders for phosphates examined by Cruickshank (1961).

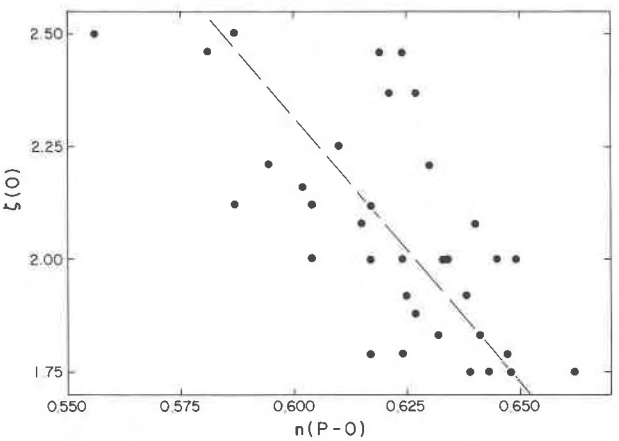

FIG. 10. Scatter diagram of n(P–O) *vs* ζ(O), the sum of the electrostatic bond strengths received by oxygen. Data from Table 1.

is not entirely surprising as the correlations between ζ(O), n[P–O] and π-bond order suggest that bond-strength parameters of both models measure similar properties of the P–O bond. What is needed is a bonding model that takes explicit account of electrostatic interactions. Although the EHMO model is deficient in this respect, it can be useful in ordering and classifying bond length variation when the electronegativity difference between bonded atoms is not large (Allen, 1970). It is hoped that studies of this type as well as those currently underway in our laboratories using CNDO-2 theory, which includes electrostatic as well as covalent interactions, may eventually explain some of the similarities between current bonding models and in the process improve our understanding of bonding in minerals.

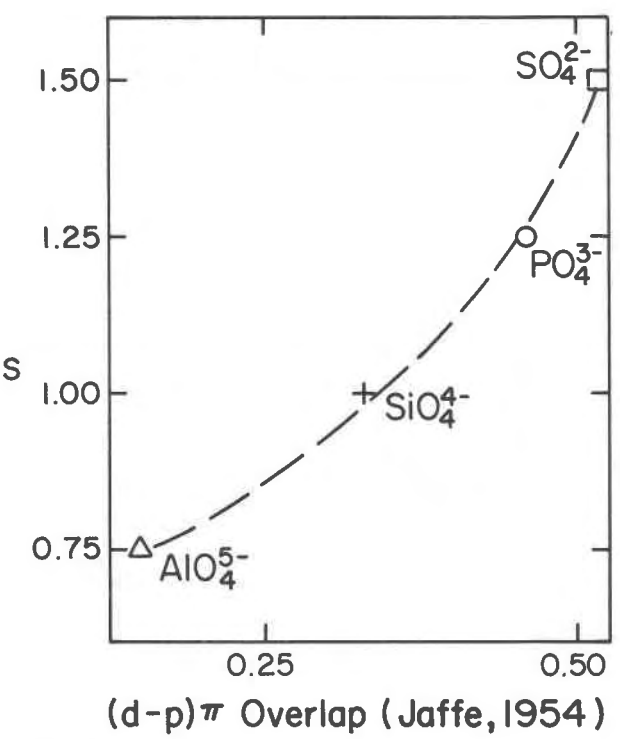

FIG. 11. Plot of the group overlap integrals (Jaffe, 1954; Brown *et al*, 1969) *vs* s, the electrostatic bond strength ($= z/\nu$ where z is the nominal charge on the cation and ν is its coordination number) for the T–O bonds in four TO_4^{n-} tetrahedral oxyanion anions.

Acknowledgments

Professors F. D. Bloss, D. W. J. Cruickshank, P. B. Moore, P. H. Ribbe, J. C. Schug, D. R. Waldbaum, and Dr. S. J. Louisnathan read the manuscript and made several helpful comments. Special thanks are due to Professor Leland C. Allen of the Chemistry Department at Princeton University, Princeton, New Jersey, for a valuable discussion of the strengths, weaknesses and the limitations of EHMO theory.

References

ALLEN, L. C. (1970) Why three-dimensional Hückel theory works and where it breaks down. *In* O. Sinanoglu and K. B. Wiberg, Eds., *Sigma Molecular Orbital Theory*, Yale Univ. Press, New Haven, Connecticut, pp. 227–248.

BARTELL, L. S., L. S. SU, AND H. YOW (1970) Lengths of phosphorus-oxygen and sulfur-oxygen bonds. An extended Hückel molecular orbital examination of Cruickshank's d_π–p_π picture. *Inorg. Chem.* **9,** 1903–1912.

BAUR, W. (1970) Bond length variation and distorted coordination polyhedra in inorganic crystals. *Trans. Amer. Crystallogr. Ass.* **6,** 125–155.

BROWN, G. E., G. V. GIBBS, AND P. H. RIBBE (1969) The nature and variation in length of the Si–O and Al–O bonds in framework silicates. *Amer. Mineral.* **54,** 1044–1061.

———, AND ——— (1970) Stereochemistry and ordering in the tetrahedral portion of silicates. *Amer. Mineral.* **55,** 1587–1607.

BROWN, I. D., AND R. D. SHANNON (1973) Empirical bond strength-bond length curves for oxides. *Acta Crystallogr.* **A29,** 266–282.

CALVO, CRISPIN (1965a) Refinement of the crystal structure of β-$Mg_2P_2O_7$. *Can. J. Chem.* **43,** 1139–1146.

——— (1965b) The crystal structure and phase transitions of β-$Zn_2P_2O_7$. *Can. J. Chem.* **43,** 1147–1153.

——— (1967) The crystal structure of α-$Mg_2P_2O_7$. *Acta Crystallogr.* **23,** 289–295.

——— (1968) The crystal structure of α-$Ca_2P_2O_7$. *Inorg. Chem.* **7,** 1345–1351.

CRUICKSHANK, D. W. J. (1961) The role of 3*d*-orbitals in π-bonds between (a) silicon, phosphorus, sulfur, or chlorine and (b) oxygen or nitrogen. *J. Chem. Soc.* **1961,** 5486–5504.

——— (1964a) Refinements of structures containing bonds between Si, P, S, or Cl and O or N. II, $Na_4P_2O_7 \cdot 10H_2O$. *Acta Crystallogr.* **17,** 672–673.

——— (1964b) Refinements of structures containing bonds between Si, P, S, or Cl and O or N. III. $Na_5P_3O_{10}$, Phase II. *Acta Crystallogr.* **17,** 674–675.

——— (1964c) Refinements of structures containing bonds between Si, P, S, or Cl and O or N. IV. $(NH_4)_4P_4O_{12}$. *Acta Crystallogr.* **17,** 675–676.

——— (1964d) Refinements of structures containing bonds between Si, P, S, or Cl and O or N. VI. P_2O_5, Form III. *Acta Crystallogr.* **17,** 679–680.

——— (1964e) Refinements of structures containing bonds between Si, P, S, or Cl and O or N. VII. $(RbPO_3)_x$. *Acta Crystallogr.* **17,** 681–682.

DICKENS, B., AND W. E. BROWN (1971) The crystal structure of $Ca_7Mg_6(Ca,Mg)_2(PO_4)_{12}$. *Tschermaks Mineral. Petrogr. Mitt.* **16,** 79–104.

GIBBS, G. V., M. M. HAMIL, S. J. LOUISNATHAN, L. S. BARTELL, AND H. YOW (1972) Correlations between Si–O bond length, Si–O–Si angle and bond overlap populations calculated using extended molecular orbital theory. *Amer. Mineral.* **57,** 1578–1613.

HOFFMANN, R. (1963) An extended Hückel theory. I. Hydrocarbons. *J. Chem. Phys.* **39,** 1397–1412.

JAFFE, H. H. (1954) Studies in molecular orbital theory. III. Multiple bonds involving *d*-orbitals. *J. Phys. Chem.* **58,** 185–190.

JARCHOW, O. H. (1964) Die Strukturverfeinerung der Zweidimensional fehlgeorgneten Natriummetaphosphates, $Na_2H_2P_4O_{12}$. *Acta Crystallogr.* **17,** 1253–1262.

LAGER, G. A. (1972) *Effect of O–P–O and P–O–P angle variations on P–O bond overlap population for some selected ortho- and pyrophosphates.* M.S. Thesis, Virginia Polytechnic Institute and State University, Blacksburg, Virginia.

———, AND G. V. GIBBS (1972) Effect of O–P–O and P–O–P angle variations on P–O bond overlap population for some selected ortho- and pyrophosphates. [abstr.] *Geol. Soc. Amer. Abstr. Programs,* **4,** 571.

LOUISNATHAN, S. J., AND G. V. GIBBS (1972) The effect of tetrahedral angles on the Si–O bond overlap population in isolated tetrahedra. *Amer. Mineral.* **57,** 1614–1642.

MCADAM, A., K. H. JEST, AND B. BEAGLEY (1968) Refinement of the structure of sodium kunol salt $(NaPO_3)_x$, Type A. *Acta Crystallogr.* **B24,** 1621–1622.

MULLIKEN, R. S. (1955) Electronic population analysis on LCAO-MO molecular wave functions. I. *J. Chem. Phys.* **23,** 1833–1846.

ONDIK, H. M. (1964) The structure of the triclinic form of sodium tetrametaphosphate tetrahydrate. *Acta Crystallogr.* **17,** 1139–1145.

PANT, A. K., AND D. W. J. CRUICKSHANK (1967) A reconsideration of the structure of datolite, $CaBSiO_4(OH)$. *Z. Kristallogr.* **125,** 286–297.

PAULING, L. (1929) The principles determining the structure of complex ionic crystals. *J. Amer. Chem. Soc.* **51,** 1010–1026.

——— (1939) *The Nature of the Chemical Bond,* 1st ed. Cornell Univ. Press, Ithaca, New York.

ROBERTSON, B. E., AND C. CALVO (1967) The crystal structure and phase transformation of α-$Ca_2P_2O_7$. *Acta Crystallogr.* **22,** 665–672.

WEBB, N. C. (1966) The crystal structure of β-$Ca_2P_2O_7$. *Acta Crystallogr.* **21,** 942–948.

Manuscript received, October 10, 1972;
accepted for publication, March 7, 1973.